Destabilization of magnetosonic-whistler waves by a relativistic runaway beam

T. Fülöp
Department of Radio and Space Science, Chalmers University of Technology, Göteborg, Sweden

G. Pokol
Department of Radio and Space Science, Chalmers University of Technology, Göteborg, Sweden and Department of Nuclear Techniques, Budapest University of Technology and Economics, Association EURATOM, Budapest, Hungary

P. Helander
EURATOM/UKAEA Fusion Association, Culham Science Centre, Abingdon, United Kingdom

M. Lisak
Department of Radio and Space Science, Chalmers University of Technology, Göteborg, Sweden

(Received 20 April 2006; accepted 5 May 2006; published online 12 June 2006)

Magnetosonic-whistler waves may be destabilized by runaway electrons both in fusion and astrophysical plasmas. A linear instability growth rate of these waves in the presence of a runaway avalanche is calculated both perturbatively and by numerical solution of the full dispersion equation. The local threshold of the instability depends on the fraction of runaways, the magnetic field, and the temperature of the background plasma. The quasilinear analysis shows that the main result of the instability is the scattering of the electrons in pitch-angle. It appears possible that this instability could explain why the number of runaway electrons generated in tokamak disruptions depends on the strength of the magnetic field. © *2006 American Institute of Physics*. [DOI: 10.1063/1.2208327]

I. INTRODUCTION

During the current quench in a tokamak disruption, a large toroidal electric field is induced, which sometimes generates a beam of highly relativistic runaway electrons with energy of order 20 MeV. These energetic electrons can cause damage to the wall, which is a potentially serious problem for reactor-scale tokamaks with large currents. In such devices, it is expected that the runaway beam may form particularly easily because of the efficacy of the so-called "runaway avalanche" mechanism.[1] In a runaway avalanche, existing runaway electrons generate new ("secondary") ones in collisions at close range with thermal electrons. The strength of the avalanche increases exponentially with the plasma current, and will be the dominant mechanism in the next generation of tokamaks.

In present experiments, up to about a half the predisruption current can be converted to runaways, and it is feared that this fraction will rise in future devices because of avalanching.[2] However, it is observed the number of runaway electrons generated varies widely between different disruptions for reasons that are not understood. In particular, several tokamaks have reported that no runaway generation occurs unless the magnetic field exceeds 2.2 T.[3–5] In the present paper, we explore a possible reason for this observation.

The runaway beam has a strongly anisotropic velocity distribution function and may excite various kinetic instabilities. Previous work has analyzed a number of such possible instabilities using simple models for the runaway distribution function. Resonant interaction of runaways with lower-hybrid waves was investigated in Refs. 6–8, and the instability threshold of the upper-hybrid wave driven unstable by runaways was derived in Ref. 9, where it was concluded that this wave is stable in collisional postdisruption plasmas.

We analyze the linear instability of magnetosonic-whistler waves destabilized by secondary runaways at Doppler-shifted harmonics of the cyclotron frequency. The unstable wave frequency will be shown to be well below the nonrelativistic electron cyclotron frequency ω_{ce} but above the ion cyclotron frequency ω_{ci}. The most important resonant interaction occurs when $\omega - k_{\|} v_{\|} = -\omega_{ce}/\gamma$ (anomalous Doppler resonance), where ω is the wave frequency, $k_{\|}$ and $v_{\|}$ are the wave number and particle velocity parallel to the magnetic field, respectively, and γ is the relativistic factor. The free-energy source driving the instability is the anisotropy of the electron distribution caused by the electric field accelerating the runaway electrons. When the degree of anisotropy exceeds a critical level, unstable waves are excited at the anomalous Doppler resonance, and the interaction with these waves leads to pitch-angle scattering of resonant electrons. As in Ref. 9, we assume that the dominant damping mechanism in the cold postdisruption plasma is collisional damping, which then determines the instability threshold. Instability of the magnetosonic-whistler waves was also considered in Refs. 10–12, but these works assumed different runaway distribution functions and different damping mechanisms. Reference 10 considers nonrelativistic electrons, Ref. 11 considers a distribution function relevant to primary (Dreicer) generation of runaways. Reference 12 considers a relativistic bi-Maxwellian distribution with temperature anisotropy, both with and without drift velocity along the magnetic field. These runaway distributions are applicable for magnetospheric plasmas, but not for tokamak disruptions.

The structure of the paper is the following. In Sec. II the kinetic equation and the secondary runaway electron distribution are presented. Section III derives the instability growth rate both perturbatively and numerically, and the threshold of the instability is investigated. Section IV analyzes the quasilinear evolution of the instability. Finally, the results are summarized in Sec. V.

II. RUNAWAY DISTRIBUTION FUNCTION

In this section we derive the velocity-space distribution function for runaway electrons produced by avalanching. As shown by Rosenbluth and Putvinski,[1] the runaway density n_r increases according to

$$\frac{dn_r}{dt} = \frac{n_r(E-1)}{c_Z\tau} \tag{1}$$

during an avalanche. Here, $\tau = 4\pi\epsilon_0^2 m_{e0}^2 c^3/n_e e^4 \ln\Lambda$ is the collision time for relativistic electrons, c the speed of light, m_{e0} the electron rest mass, n_e the background electron density, $E = e|E_\parallel|\tau/m_{e0}c$ the normalized parallel electric field, $c_Z = \sqrt{3(Z+5)/\pi}\ln\Lambda$, and Z the effective ion charge.

The distribution function is calculated from the kinetic equation for relativistic electrons in a homogeneous magnetic field:

$$\tau\frac{\partial f}{\partial t} + E\frac{\partial f}{\partial p_\parallel} \simeq \frac{1}{p^2}\frac{\partial}{\partial p}(1+p^2)f + \frac{1+Z}{p^3}\sqrt{1+p^2}\mathcal{L}(f), \tag{2}$$

where $p = \gamma v/c$ is the normalized relativistic momentum, $\gamma = \sqrt{1+p^2}$ the Lorentz factor, and

$$\mathcal{L} = \frac{1}{2}\frac{\partial}{\partial\xi}(1-\xi^2)\frac{\partial}{\partial\xi} \tag{3}$$

the scattering operator, with $\xi = p_\parallel/p$ the pitch-angle variable. In a tokamak disruption $E \gg 1$, and the runaway tail has the character of a beam, so that the parallel momentum is much larger than the perpendicular: $p_\perp \ll p_\parallel \simeq p$. The kinetic equation then reduces to

$$\tau\frac{\partial f}{\partial t} + (E-1)\frac{\partial f}{\partial p_\parallel} = \frac{1+Z}{2}\frac{1}{p_\perp}\frac{\partial}{\partial p_\perp}p_\perp\frac{\partial f}{\partial p_\perp}. \tag{4}$$

Denoting the distribution function over $p_\parallel$ by

$$F(p_\parallel,t) = \int_0^\infty f(p_\parallel,p_\perp,t)2\pi p_\perp dp_\perp \tag{5}$$

and integrating Eq. (4) over $p_\perp$ gives

$$\tau\frac{\partial F}{\partial t} + (E-1)\frac{\partial F}{\partial p_\parallel} = 0. \tag{6}$$

The solution to this equation that satisfies Eq. (1) is

$$F(p_\parallel,t) = \exp\left(\frac{(E-1)t/\tau - p_\parallel}{c_Z}\right), \tag{7}$$

and the solution to Eq. (4) can be constructed as $f(p_\parallel,p_\perp,t) = F(p_\parallel,t)g(p_\parallel,p_\perp)$, where g satisfies the diffusion equation

$$(E-1)\frac{\partial g}{\partial p_\parallel} = \frac{1+Z}{2p_\perp}\frac{\partial}{\partial p_\perp}p_\perp\frac{\partial g}{\partial p_\perp}. \tag{8}$$

Since runaways are generated in a beam at low p, the appropriate solution of this equation is the usual Gaussian, and the distribution function becomes

$$f(p_\parallel,p_\perp,t) = \frac{C}{p_\parallel}\exp\left(\frac{(E-1)t/\tau - p_\parallel}{c_Z} - \frac{\alpha p_\perp^2}{2p_\parallel}\right), \tag{9}$$

where $\alpha = (E-1)/(1+Z)$ and C is related to the runaway density by

$$C = \frac{n_r\alpha}{2\pi c_Z}\exp\left[\frac{(E-1)t}{\tau c_Z}\right].$$

III. STABILITY ANALYSIS

The dispersion relation for the fast wave is

$$(\epsilon_{11} - k_\parallel^2c^2/\omega^2)(\epsilon_{22} - k^2c^2/\omega^2) + \epsilon_{12}^2 = 0, \tag{10}$$

where k is the wave number and $\boldsymbol{\epsilon} = \mathbf{1} + \boldsymbol{\chi}$ is the dielectric tensor[13] consisting of contributions from cold background ions, electrons, and energetic runaway electrons. For the frequency range $\omega_{ci} \ll \omega \ll \omega_{ce}$, the background ion and electron contributions to $\boldsymbol{\chi}$ are

$$\chi_{11}^i = -\frac{\omega_{pi}^2}{\omega^2}, \quad \chi_{22}^i = -\frac{\omega_{pi}^2}{\omega^2}, \quad \text{and} \quad \chi_{12}^i = i\frac{\omega_{pi}^2\omega_{ci}}{\omega^3}, \tag{11}$$

$$\chi_{11}^e = \frac{\omega_{pe}^2}{\omega_{ce}^2}, \quad \chi_{22}^e = \frac{\omega_{pe}^2}{\omega_{ce}^2}, \quad \text{and} \quad \chi_{12}^e = i\frac{\omega_{pe}^2}{\omega\omega_{ce}}, \tag{12}$$

where ω_{pi} and ω_{pe} are the ion and electron plasma frequencies, respectively, and $k_\perp$ is the component of the wave vector perpendicular to the magnetic field, and we assumed $k_\perp^2 v_{Te}^2 \ll \omega^2$, where v_{Te} is the electron thermal speed. Assuming $|k| \gg |k_\parallel|$ and $\omega_{pi}^2 \ll k^2c^2 \ll \omega_{pe}^2$, the dispersion relation can be simplified to

$$k^2v_A^2\left(1 + \frac{k_\parallel^2c^2}{\omega_{pi}^2}\right) - \omega^2 = \frac{\omega_{ci}^2\omega^2}{\omega_{pi}^2}\left[\left(1 + \frac{k^2v_A^2}{\omega_{ci}^2}\right)\chi_{11}^r + \left(1 + \frac{k_\parallel^2v_A^2}{\omega_{ci}^2}\right)\chi_{22}^r - 2i\frac{\omega}{\omega_{ci}}\chi_{12}^r\right], \tag{13}$$

where $v_A = c\omega_{ci}/\omega_{pi}$ is the Alfvén velocity and the superscript "r" denotes the runaway contribution to the dielectric tensor. Without runaways, this equation gives the magnetosonic-whistler dispersion relation $\omega_0 = kv_A\sqrt{1 + k_\parallel^2c^2/\omega_{pi}^2}$, which reduces to the magnetosonic wave $\omega_0 = kv_A$ for perpendicular propagation ($k_\parallel = 0$) and to the whistler wave $\omega_0 = kk_\parallel v_A^2/\omega_{ci}$ for $k_\parallel^2c^2/\omega_{pi}^2 \gg 1$. In the frequency range of interest, the χ_{22}^r or $i\chi_{12}^r$ terms can be neglected if $k^2v_A^2 \gg \omega\omega_{ci}$ and the dispersion relation then takes the following form:

$$k^2 v_A^2\left(1+\frac{k_\parallel^2 c^2}{\omega_{pi}^2}\right)-\omega^2=\omega^2\frac{k^2 v_A^2}{\omega_{pi}^2}\chi_{11}^r. \tag{14}$$

The remaining runaway contribution to the dielectric tensor is

$$\chi_{11}^r=2\pi\frac{\omega_{pr}^2\omega_{ce}^2}{k_\perp^2\omega c^2}\times\int_0^\infty dp_\perp\int_{-\infty}^\infty dp_\parallel\sum_{n=-\infty}^{\infty}\frac{U}{\gamma(\omega-k_\parallel c p_\parallel/\gamma-n\Omega)}n^2J_n^2(z), \tag{15}$$

where $\omega_{pr}=\sqrt{n_r e^2/m_{e0}\epsilon_0}$ is the nonrelativistic runaway electron plasma frequency, J_n is the Bessel function of the first kind and of order n, $\Omega=eB/m_e=\omega_{ce}/\gamma$, $z=k_\perp c p_\perp/\omega_{ce}$, and

$$U=\frac{\partial f_r}{\partial p_\perp}+\frac{k_\parallel c}{\omega\gamma}\left(p_\perp\frac{\partial f_r}{\partial p_\parallel}-p_\parallel\frac{\partial f_r}{\partial p_\perp}\right), \tag{16}$$

where $f_r=f/n_r$ is the normalized runaway distribution function. The instability growth rate can be calculated by solving (14) for the runaway distribution (9).

A. Perturbative analysis

The instability growth rate for a small perturbation $\omega=\omega_0+\delta\omega$, where $\gamma_i=\mathrm{Im}\,\delta\omega$, is given by

$$\frac{\gamma_i}{\omega_0}=-\frac{k^2v_A^2}{2\omega_{pi}^2}\,\mathrm{Im}\,\chi_{11}^r=\frac{\pi^2\omega_{pr}^2}{\omega_{pi}^2}\frac{k^2v_A^2}{\omega_0^2}\frac{\omega_{ce}^2}{k_\perp^2c^2}\frac{1}{k_\parallel c}\times\int_0^\infty dp_\perp\int_{-\infty}^\infty dp_\parallel\sum_{n=-\infty}^{\infty}n^2J_n^2(z)\delta[p_\parallel+(n\Omega-\omega_0)\gamma/(k_\parallel c)]\times\left(\frac{n\omega_{ce}}{\gamma}\frac{\partial f_r}{\partial p_\perp}+\frac{k_\parallel c p_\perp}{\gamma}\frac{\partial f_r}{\partial p_\parallel}\right). \tag{17}$$

For the ultrarelativistic runaway tail $\gamma\simeq p_\parallel$, and the resonance condition gives $p_\parallel=p_{\mathrm{res}}\equiv-n\omega_{ce}/(k_\parallel c-\omega_0)$, which allows us to evaluate the $p_\parallel$ integral and to obtain

$$\frac{\gamma_i}{\omega_0}=\frac{\pi^2\omega_{pr}^2}{\omega_{pi}^2}\frac{k^2v_A^2}{\omega_0^2}\frac{\omega_{ce}^2}{k_\perp^2c^2}\frac{1}{1-y}\times\int_0^\infty dp_\perp\sum_{n=-\infty}^{\infty}n^2J_n^2\left(\frac{n\omega_{ce}}{k_\parallel cp_\parallel}\frac{\partial f_r}{\partial p_\perp}+\frac{p_\perp}{p_\parallel}\frac{\partial f_r}{\partial p_\parallel}\right)\Bigg|_{p_\parallel=p_{\mathrm{res}}}, \tag{18}$$

where $y=\omega_0/k_\parallel c$.

B. Secondary runaway instability

Substituting the runaway electron distribution from Eq. (9) into the expression for γ_i and evaluating the derivatives, we obtain

$$\frac{\gamma_i}{\omega_0}=\hat{C}\sum_{n=-\infty}^{\infty}\int_0^\infty p_\perp dp_\perp n^2J_n^2(K_\perp p_\perp)\times\exp(a_n p_\perp^2)[b_n+a_n(1-y)K_\parallel p_\perp^2/n] \tag{19}$$

where $K_\perp=k_\perp c/\omega_{ce}$, $K_\parallel=k_\parallel c/\omega_{ce}$,

$$a_n=\frac{\alpha K_\parallel(1-y)}{2n},\quad b_n=\alpha(1-y)+\frac{K_\parallel(1-y)}{n}-\frac{1}{c_Z},$$

and

$$\hat{C}=(1-y)\frac{\pi\alpha\omega_{pr}^2}{2c_Z\omega_{pi}^2}\frac{k^2v_A^2}{\omega_0^2}\frac{k_\parallel^2}{k_\perp^2}\exp\left\{\frac{n/[K_\parallel(1-y)]}{c_Z}\right\}.$$

Note that the $n=0$, resonance will not contribute. For realistic parameters and the frequency region of interest ($\omega_{ci}\ll\omega_0\ll\omega_{ce}$), only the anomalous Doppler resonance ($n=-1$) has to be taken into account. Keeping only the $n=-1$ resonance gives

$$\frac{\gamma_i}{\omega_0}=\frac{\hat{C}}{4a_{-1}^2}\{K_\perp^2K_\parallel(1-y)I_0(\lambda)+[2a_{-1}b_{-1}+K_\perp^2K_\parallel(1-y)]I_1(\lambda)\}e^\lambda, \tag{20}$$

where $\lambda=K_\perp^2/(2a_{-1})$, I_n are modified Bessel functions of the first kind and of order n. Assuming that $\lambda\ll1$, we can expand the Bessel and exponential functions for small parameters, so that the growth rate becomes

$$\frac{\gamma_i}{\omega_0}=\frac{\pi}{4c_Z}\frac{\omega_{pr}^2}{\omega_{pi}^2}\frac{k^2v_A^2}{\omega_0^2}\frac{\alpha+K_\parallel}{\alpha}\exp\left[\frac{-\omega_{ce}}{(k_\parallel c-\omega_0)c_Z}\right], \tag{21}$$

and if we furthermore assume $\alpha\gg K_\parallel$, it simplifies to

$$\gamma_i(\omega_0,k,k_\parallel)=\frac{\pi}{4c_Z}\frac{\omega_{pr}^2}{\omega_{pi}^2}\frac{k^2v_A^2}{\omega_0}\exp\left[\frac{-\omega_{ce}}{(k_\parallel c-\omega_0)c_Z}\right] \tag{22}$$

to the lowest order in λ. At low frequencies, the growth rate increases monotonically, and at higher frequencies we can use the whistler branch of the dispersion relation ($\omega_0=kk_\parallel v_Ac/\omega_{pi}$). The growth rate of the fastest growing wave can be obtained using the condition $\partial\gamma_i(k_\parallel,k)/\partial k_\parallel=0$, leading to $c_Zk_\parallel c(1-kv_A/\omega_{pi})=\omega_{ce}$. This condition can be used with (22) to derive the maximum growth rate:

$$\gamma_i(k_\parallel)=\frac{\pi}{4c_Z}\frac{\omega_{pr}^2}{k_\parallel c}\left(1-\frac{\omega_{ce}}{c_Zk_\parallel c}\right)\exp(-1). \tag{23}$$

The $\gamma_i(k_\parallel)$ function has a maximum, determined by the $\partial\gamma_i/\partial k_\parallel=0$ condition, giving $k_\parallel c=2\omega_{ce}/c_Z$, so that

$$\gamma_i^{\max}=\frac{\pi}{16}\frac{\omega_{pr}^2}{\omega_{ce}}\exp(-1)=1.3\times10^{-9}\frac{n_r}{B_T} \tag{24}$$

(where B_T denotes B in Tesla) is the growth rate of the most unstable mode. Note that the dependence on electric field is solely contained in the number of runaway electrons n_r derived in Sec. II. To obtain Eq. (24), we have made the following assumptions: $|k|\gg|k_\parallel|$, $\omega_{ci}\ll\omega_0\ll\omega_{ce}$, $\lambda\ll1$, $k_\parallel^2c^2/\omega_{pi}^2\gg1$, $k_\perp^2v_{Te}^2\ll\omega^2$, $\omega\omega_{ci}\ll k^2v_A^2\ll\omega_{ci}\omega_{ce}$, and $\alpha\gg K_\parallel$. The most unstable wave has the wave number $kv_A/\omega_{pi}=1/2$, the parallel wave number $k_\parallel c=2\omega_{ce}/c_Z$, and the wave frequency $\omega_0=\omega_{ce}/c_Z$, so that the assumptions above are clearly satisfied.

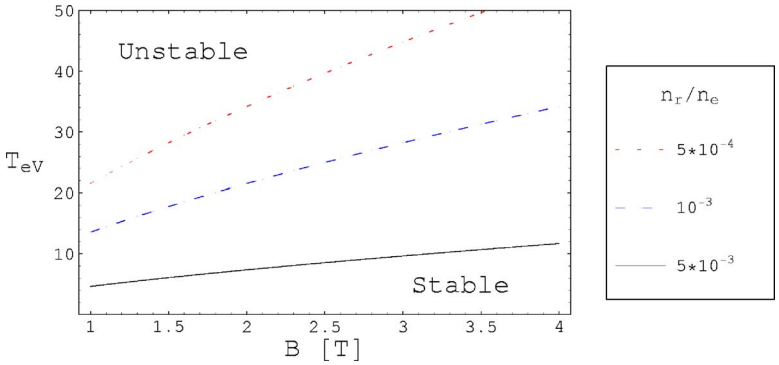

FIG. 1. (Color online) Stability threshold from Eq. (25) for different runaway fractions.

C. Instability threshold

To determine the instability threshold, we must compare the growth rate with the damping due to electron-ion collisions. Reference 14 shows that electron-electron collisions do not contribute to the collisional damping and ion-electron collisions can be accounted for by adding to the wave frequency an imaginary part $\omega \rightarrow \omega - i1.5\tau_{ei}^{-1}$, corresponding to a damping rate $\gamma_d = -1.5\tau_{ei}^{-1}$, where the electron-ion collision time is $\tau_{ei} = 3\pi^{3/2} m_{e0}^2 v_{Te}^3 \epsilon_0^2 / n_i Z^2 e^4 \ln\Lambda$. The threshold $\gamma_i > \gamma_d$ can be written as

$$\frac{n_r}{n_e} > \frac{Z^2 B_T}{20 T_{\mathrm{eV}}^{3/2}}, \tag{25}$$

where T_{eV} is the background plasma temperature in eV and n_r/n_e is the fraction of the runaways. This inequality is the local threshold for the instability of the magnetosonic-whistler wave, where every quantity is to be understood at a given location.

It is clear from (25) that collisional damping is less effective for high temperature plasmas, and therefore the runaway density that is needed for driving the mode unstable is smaller. This may indicate that this instability will arise quite early in the thermal quench. However, this effect may be counterbalanced by the fact that the n_r/n_e runaway fraction grows exponentially with time. The temporal evolution of the threshold depends sensitively on the evolution of the different plasma parameters, and it is not discussed further.

The threshold (25) does not depend on the plasma density, only the fraction of the runaways is important. The critical runaway fraction grows with magnetic field strength, so that the magnetosonic-whistler wave is more easily destabilized for low magnetic fields. Figure 1 illustrates the threshold in plasma temperature as a function of the toroidal magnetic field strength for different runaway ratios. In this and later figures, we show calculations for pure deuterium plasma ($m_i = 2m_p$, $Z=1$).

D. Numerical analysis

The perturbative analysis described in the previous subsections is complemented by a numerical analysis. First, the runaway contribution to the susceptibility tensor was evaluated for relevant plasma parameters by numerically integrating expression (15) (and similar expressions for χ_{22}^r and χ_{12}^r, which are not given here but can be found in Ref. 13). As expected, Re χ_{11}^r, Re χ_{22}^r, and Im χ_{12}^r have been found to be negligible compared to the background electron and ion contributions to the susceptibility tensor for all resonances and for runaway fractions up to 10^{-2}. The tensor elements are largest for $n = \pm 1$, and in our case only the anomalous Doppler resonance ($n=-1$) contributes to the growth rate. Numerical integration of Im χ_{11}^r, Im χ_{22}^r, and Re χ_{12}^r confirms that the assumptions leading to Eq. (14) are satisfied.

The results of the perturbative stability analysis are confirmed by the numerical solution of the full dispersion relation. To this end, Eq. (10) has been solved with a damped Newton's method, with the starting point derived from the analytical solution. In cases when this method has convergence problems, a variant of the secant method was used with varying step lengths and linear extrapolation to determine the starting direction. The analytically derived magnetosonic-whistler dispersion relation was checked against the numerical solution of the dispersion relation ex-

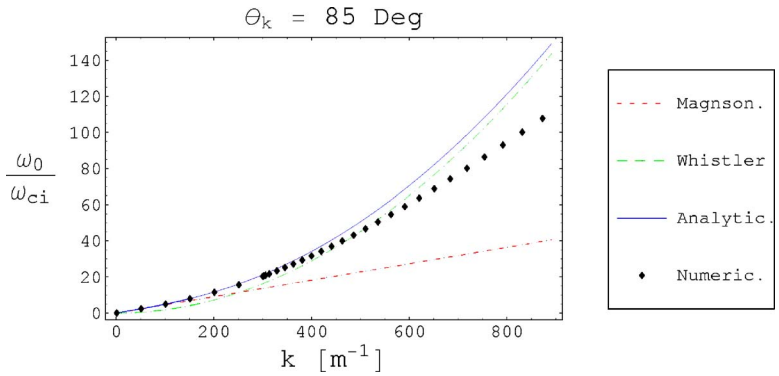

FIG. 2. (Color online) Comparison of numerical and analytical dispersion relations for a fixed angle of propagation ($n_e = 5\times10^{19}$ m^{-3}, $B=2$ T, and $T=10$ eV deuterium plasma).

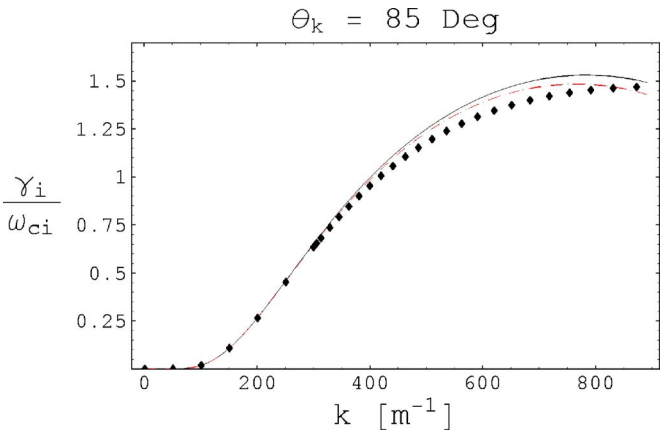

FIG. 3. (Color online) Comparison of numerical and analytical growth rates as a function of wave number ($n_e=5\times10^{19}$ m^{-3}, $B=2$ T, $T=10$ eV, and $n_r/n_e=5\times10^{-3}$, deuterium plasma). The solid line corresponds to Eq. (22), the dashed line is Eq. (20), and the diamonds are the numerical result obtained by solution of the dispersion relation.

cluding the runaway susceptibility term, but using the full hot plasma susceptibility[13] for both ions and electrons instead of Eqs. (11) and (12).

Figure 2 shows the results of the analytical and the numerical dispersion relation together with the two approximations: the magnetosonic-wave dispersion for low frequency limit and the whistler-wave dispersion for the high frequency limit. The dispersion relations are plotted assuming a fixed angle of propagation ($\theta_k=85°$). This angle will be shown to be close to the propagation angle, giving the maximum growth rate for the set of plasma parameters used. The deviation of the analytical and numerical values at higher wave numbers is due to the neglect of the identity tensor and the electron contributions χ^e_{11} and χ^e_{22} in the dielectric tensor.

Growth rates calculated from the perturbative analysis [Eqs. (20) and (22)] were also compared to numerical results by solving the dispersion relation, including the imaginary part of the most important runaway susceptibility term ($\mathrm{Im}\,\chi^r_{11}$) in the dielectric tensor and the full hot plasma susceptibility.[13] Figure 3 shows the numerical and analytical growth rates as functions of the wave number. The growth rate has a maximum for the propagation angle $\theta=85°$, and the analytical and numerical values for the growth rate are in reasonable agreement. The analytical growth rates calculated from the perturbative analysis are in good agreement. The discrepancy is caused by the deviation of the real part of the frequency.

Next, we investigate the dependence of the growth rate on plasma parameters. The scaling of growth rate with respect to the magnetic field is the most interesting since experimental observations suggest that the number of runaways generated in a disruption is dependent on the magnetic field strength. Normalized growth rates as a function of propagation angle for different magnetic field strengths are presented in Fig. 4, where the threshold corresponds to $\gamma_i/\gamma_d-1=0$. Note that only waves with $|k|\gg|k_\parallel|$ are unstable, as was assumed in Sec. III. In the region of validity and for propagation angles close to perpendicular, the numerical results lie close to the analytical ones.

As expected from the analytical expression for the threshold [Eq. (25)], Fig. 5 shows that the maximum normalized growth rates are not sensitive to the plasma density. For lower densities, however, the maximum of the growth rate shifts towards larger $k_\parallel$, making our assumption $|k_\parallel|\ll|k|$ invalid. Therefore, at low density, our conclusions about the maximum growth rate do not hold.

Figure 6 presents the scaling of growth rate with temperature. As already discussed, the normalized growth rate increases with temperature, indicating a decreasing threshold. It can also be seen that the shape of the growth rate curve does not change apart from a multiplication by a constant. Numerical calculations show that finite temperature effects distort the curve at very high temperatures (around a few keV depending on the density).

IV. QUASILINEAR ANALYSIS

Beyond the linear phase of the instability, the dynamics of the resonant interaction between the electrons and waves can be described by quasilinear theory. The distribution function of the particles is then separated into a slowly and a rapidly varying part, and only the average effect of the rapidly varying part on the slowly varying part is taken into account. The slowly varying part of the distribution is then described by a diffusion equation in phase space, and the rate of growth of wave-energy is equal to the linear growth rate. The quasilinear equation for the runaway distribution is[15]

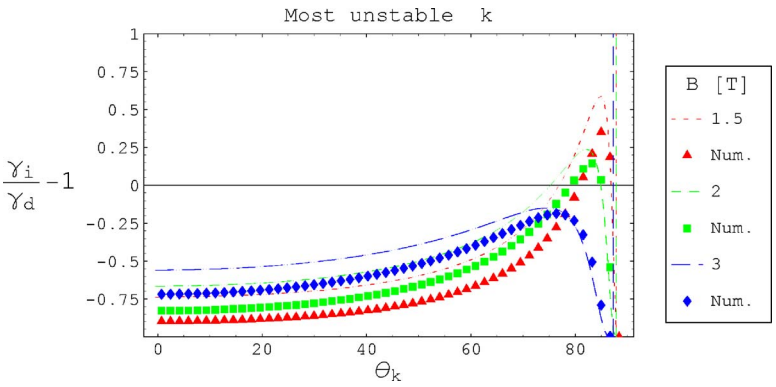

FIG. 4. (Color online) Numerical and analytical growth rates for deuterium plasma at different magnetic field strength values ($n_e=5\times10^{19}$ m^{-3}, $T=10$ eV, and $n_r/n_e=5\times10^{-3}$).

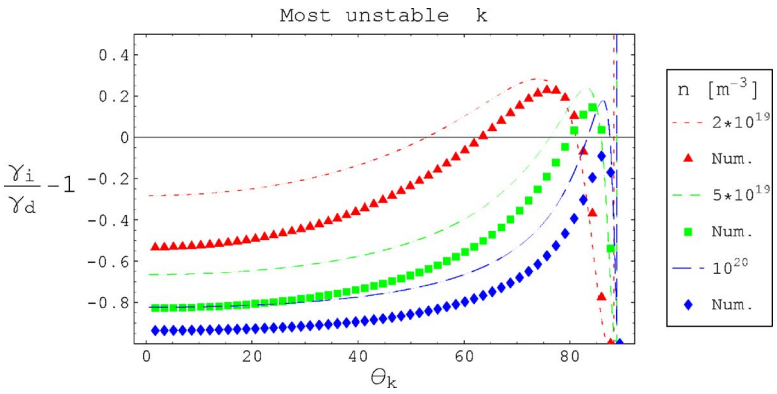

FIG. 5. (Color online) Analytical and numerical growth rates for deuterium plasma just above the threshold ($B=2$ T, $T=10$ eV, $n_r/n_e=5\times10^{-3}$).

$$\frac{\partial f}{\partial t}=\frac{\pi e^2}{m_e^2}\sum_{l=-\infty}^{\infty}\int d^3k\hat{\Pi}\frac{|E_k|^2}{k^2}J_l(z)^2\delta(\omega-l\Omega-k_\parallel p_\parallel c/\gamma)\hat{\Pi}f, \tag{26}$$

where

$$\hat{\Pi}=\frac{\omega-l\Omega}{v_\parallel}\frac{\partial}{\partial v_\parallel}+\frac{l\Omega}{v_\perp}\frac{\partial}{\partial v_\perp}, \tag{27}$$

and if we assume $\partial f/\partial v_\parallel \ll \partial f/\partial v_\perp$, for $l=-1$ and $z\ll 1$, Eq. (26) simplifies to a diffusion equation

$$\frac{\partial f(p_\perp,p_\parallel,t)}{\partial t}=\frac{1}{p_\perp}\frac{\partial}{\partial p_\perp}\left(\frac{D}{p_\perp}\frac{\partial f}{\partial p_\perp}\right) \tag{28}$$

with the diffusion constant $D=2\pi^2\omega_{ce}^2p_\perp^2c^{-2}B^{-2}\int d^3kW_kk_\perp^2k^{-2}\delta(\omega+\Omega-k_\parallel p_\parallel c/\gamma)$, where $W_k=|E_k|^2/8\pi$ is the spectral energy of the wave that is assumed to have the time variation $dW_k/dt=2\gamma_kW_k$. Introducing a time-variable

$$\tau=2\pi^2\omega_{ce}^2c^{-2}B^{-2}\int_0^t dt'\int d^3kW_k(t')k_\perp^2k^{-2}\delta \times(\omega_k+\Omega-k_\parallel p_\parallel c/\gamma), \tag{29}$$

the solution of the diffusion equation (26) with the initial value (9) is

$$f(p_\perp,p_\parallel,t)=\frac{f_0}{(2\alpha\tau/p_\parallel+1)}\exp\left(-\frac{\alpha p_\perp^2}{2(2\alpha\tau+p_\parallel)}\right) \tag{30}$$

with

$$f_0=\frac{C}{p_\parallel}\exp\left(\frac{\langle E\rangle-p_\parallel}{c_Z}\right). \tag{31}$$

Equation (30) indicates that the pitch-angle scattering increases the mean perpendicular energy linearly with time. Assuming a narrow spectrum of unstable waves centered around $k_c=\omega_{pi}/2v_A\simeq 3\times10^3n_{20}/B$ [m^{-1}] and $k_\parallel\simeq\omega_{ce}/c\ln\Lambda\simeq 30B$ [m^{-1}], we can estimate the time scale for the perpendicular energy to increase a few times. Assuming that the time-evolution of the spectral energy is $W_k(t)=\frac{1}{2}T_ee^{2\gamma_kt}$, we can solve Eq. (29) to give

$$\tau=\frac{\pi^3e^2\gamma k_c^2v_{T_e}^2}{2m_ec^3\gamma_k}e^{2\gamma_kt}, \tag{32}$$

so that the time scale for perpendicular energy increase is

$$t=\frac{1}{2\gamma_k}\ln\left(\frac{\tau\gamma_km_e^2c^3}{\pi^3e^2T_ek_c^2}\right)\simeq 3\times10^{-7}\text{ s} \tag{33}$$

for $\gamma_k\simeq10^8$ s^{-1}, $\gamma=40$, $T_e=10$ eV, and $\tau\simeq p_\parallel/(2\alpha)\simeq 0.1$.

V. CONCLUSIONS

We have analyzed the stability of magnetosonic-whistler waves in the presence of a relativistic runaway electron beam. A perturbative calculation of the growth rate agrees well with that found by a full numerical solution of the dispersion relation. The analysis is local—no spatial variation of magnetic field or plasma parameters is considered—which is justified *a posteriori* by noting that the growth rate is sufficiently large that the inequality

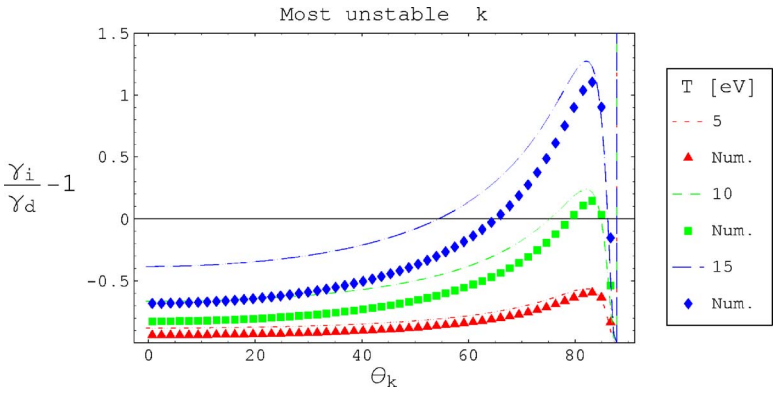

FIG. 6. (Color online) Analytical and numerical growth rates for deuterium plasma at different temperatures ($B=2$ T, $n_e=5\times10^{19}$ m^{-3}, and $n_r/n_e=5\times10^{-3}$).

$$\frac{a}{\partial\omega_k/\partial k_\perp}\gamma_k \simeq \frac{a\omega_{pi}c_Z}{v_A\omega_{ce}}\gamma_k \gg 1, \tag{34}$$

is well satisfied. Here, a denotes the radius of the runaway beam (tens of centimeters) and the left-hand side measures the number of e-foldings by which the wave is amplified as it propagates the distance a. The threshold of the instability depends on the fraction of runaways, the magnetic field, and the temperature of the background plasma:

$$\frac{n_r}{n_e} > \frac{Z^2 B_T}{20 T_{\mathrm{eV}}^{3/2}}, \tag{35}$$

but is independent of other plasma parameters. Quasilinear analysis suggests that the main result of the instability is rapid pitch-angle scattering of the resonant electrons.

We speculate that the presence of a magnetosonic-whistler wave instability may be the reason for the observation that the number of runaway electrons produced during disruptions in large tokamaks depends sensitively on the magnetic field strength. As mentioned in Sec. I, a critical toroidal magnetic field of around 2.2 T,[3–5] below which no runaway production occurs, has been reported for several devices. One reason for the absence of runaways could be that the whistler instability scatters runaways and prevents the beam from forming. The observed critical field is of the same order of magnitude as our instability threshold. Taking, for instance, a plasma density $n_e = 3\times10^{19}$ m^{-3} and a runaway current density, $j_r = n_r ec = 2$ MA/m^2, typical of JET,[16] gives a threshold temperature $T_e = 17$ eV (for $Z=1$). Experimentally, the postdisruption temperature is highly uncertain, but is commonly believed (on various grounds) to be around 10 eV. It is thus clear that the instability threshold is in the right parameter range. In contrast, Rosenbluth *et al.*[9] arrived at the condition $Z_{\mathrm{eff}}\sqrt{n_{20}}/(T_{\mathrm{eV}})^{3/2} < 0.01$ for the destabilization of the upper hybrid mode. Clearly, the upper-hybrid mode is stable for JET and ITER parameters, while the whistler wave may not be. However, in order to make a more definite judgement about the importance of the latter, it would be necessary to refine the analysis performed in the present paper. In particular, a self-consistent simulation of the runaway distribution function and electric field evolution, as achieved, for instance, by the ARENA code,[2] could be coupled to an evaluation of the instability growth rate.

Another possible application could be to discharges of the type described in Ref. 17, where it was suggested that unstable whistler waves may be responsible for the observed losses of runaway electrons. However, our theory is not immediately applicable to these discharges since the runaways are either of Dreicer origin (in so-called RAD-I discharges) or are generated by weaker electric fields than we have assumed ($E \sim 1$). A straightforward application of the criterion (35) would suggest that the waves are stable because of the low electron temperature in these plasmas.

ACKNOWLEDGMENTS

This work was funded jointly by the United Kingdom Engineering and Physical Sciences Research Council and by the European Communities under Association Contracts between EURATOM, UKAEA, HAS, and *Vetenskapsrådet*. The views and opinions expressed herein do not necessarily reflect those of the European Commission. One of the authors (G.P.) acknowledges the support of a bilateral funding of the Swedish Institute and the Hungarian Scholarship Board.

[1] M. N. Rosenbluth and S. V. Putvinski, Nucl. Fusion **37**, 1355 (1997).
[2] L.-G. Eriksson, P. Helander, F. Andersson, D. Anderson, and M. Lisak, Phys. Rev. Lett. **92**, 205004 (2004).
[3] R. D. Gill, B. Alper, M. de Baar *et al.*, Nucl. Fusion **42**, 1039 (2002).
[4] R. Yoshino, S. Tokuda, and Y. Kawano, Nucl. Fusion **39**, 151 (2000).
[5] M. Lisak, U. Schneider, G. Martin *et al.*, Nucl. Fusion **42**, 937 (2002).
[6] V. V. Parail and O. P. Pogutse, Nucl. Fusion **18**, 303 (1978).
[7] V. V. Parail and O. P. Pogutse, Rev. Plasma Phys. **11**, 1 (1986).
[8] C. S. Liu and Y. Mok, Phys. Rev. Lett. **38**, 162 (1977).
[9] M. N. Rosenbluth, P. B. Parks, D. Post, S. Putvinski, N. Putvinskaya, and H. A. Scott, in *Proceeding of the 16th International Conference on Fusion Energy, Montreal, 1996* (International Atomic Energy Agency, Vienna, 1997), Vol. 2, p. 979.
[10] C. Kennel, Phys. Fluids **9**, 2190 (1966).
[11] A. G. Elfimov and R. M. O. Galvao, Plasma Phys. Controlled Fusion **45**, L63 (2003).
[12] R. Ciurea-Borcia, G. Matthieussent, E. L. Bel, F. Simonet, and J. Solomon, Phys. Plasmas **7**, 359 (2000).
[13] T. H. Stix, *Waves in Plasmas* (AIP, Melville, NY, 1992).
[14] M. Brambilla, Phys. Plasmas **2**, 1094 (1995).
[15] M. Lisak, Phys. Scripta **29**, 87 (1984).
[16] J. A. Wesson, R. D. Gill, M. Hugon *et al.*, Nucl. Fusion **29**, 641 (1989).
[17] Yu. K. Kuznetsov, R. M. O. Galvao, V. Bellintani *et al.*, Nucl. Fusion **44**, 631 (2004).